



HAL
open science

Normal impact of a ball rotating around its linear velocity

Théophile Rémond, Vincent Dolique, Renaud Rinaldi, Jean-Christophe Géminard

► **To cite this version:**

Théophile Rémond, Vincent Dolique, Renaud Rinaldi, Jean-Christophe Géminard. Normal impact of a ball rotating around its linear velocity. *Physical Review E*, 2024, 110 (1), pp.015002. 10.1103/PhysRevE.110.015002. hal-04673325

HAL Id: hal-04673325





<https://hal.science/hal-04673325v1>

Submitted on 20 Aug 2024

HAL is a multi-disciplinary open access archive for the deposit and dissemination of scientific research documents, whether they are published or not. The documents may come from teaching and research institutions in France or abroad, or from public or private research centers.

L'archive ouverte pluridisciplinaire **HAL**, est destinée au dépôt et à la diffusion de documents scientifiques de niveau recherche, publiés ou non, émanant des établissements d'enseignement et de recherche français ou étrangers, des laboratoires publics ou privés.

Normal impact of a ball rotating around its linear velocity

Théophile Rémond ¹, Vincent Dolique ¹, Renaud G. Rinaldi ² and Jean-Christophe Géminard ¹

¹*LPENSL, CNRS UMR5672, ENS de Lyon, Université Lyon, F-69342 Lyon, France*

²*MATEIS, CNRS UMR 5521, INSA-Lyon, Université Lyon, F-69621 Villeurbanne, France*



(Received 17 January 2024; revised 3 June 2024; accepted 26 June 2024; published 30 July 2024)

We report on an experimental study of the normal impact on a solid surface of a table tennis ball that rotates around its linear velocity vector. We observe that the ratio of the reflected velocity to the incident velocity does not depend on the initial spin. In contrast, the reflected spin depends not only on the incident spin but also on the incident velocity. The experimental results, which reveal the tricky role played by the friction in the region of contact, are accounted for by simple theoretical arguments.

DOI: [10.1103/PhysRevE.110.015002](https://doi.org/10.1103/PhysRevE.110.015002)

I. INTRODUCTION

For practical reasons, the impact of solid objects has long attracted lots of attention. A reliable description of the collision law is mandatory if one needs to accurately describe systems like granular materials, to only cite one important field of application [1]. In the same way, the rebound of sport balls has attracted the attention of a rather large community, either for educational purposes or practical applications. Indeed, even if the problem can be tackled with simple tools of classical mechanics, the results are interesting, in particular for those who need laws as input in numerical simulations, for instance.

The first relevant property of the rebound of sports balls on a surface, field, or racket is the restitution of the normal linear velocity (the ratio, along the normal to the surface, of the reflected velocity to the incident velocity) which accounts for the energy loss during the contact. Under normal incidence, the determination of the restitution coefficient, for both full and hollow spheres, has been the subject of several studies [2–7]. When it comes to the impact with a racket, the players tend to call their equipment fast or slow, with such qualifier being directly related to the value of this restitution coefficient.

The second relevant property of the rebound is the ability of the ball to gain or lose spin during the collision. Again many studies have focused on the change in the angular velocity of the ball during the collision [3–5,8–14]. One important result for a table tennis ball is that, for an impact with a solid substrate, the kinematics of the ball only depends on the restitution coefficient of the normal velocity and on the frictional coefficient which accounts for the contact between the surfaces [7]. The spin given by the racket will make it suitable for different playing styles, from offensive to defensive.

In spite of the consequent effort, none of the former studies considered the case of a ball, spinning around its linear velocity, impinging in normal incidence on a flat and rigid surface. Even if the configuration can seem, at first sight, to be very specific, it is, as a matter of fact, quite general. Indeed, for a ball impinging in oblique incidence with a random spin, the component of the angular velocity perpendicular to the

surface is most likely nonzero. It turns out that none of the existing models can predict how this component of the angular velocity is altered by the collision.

Imagine thus that a ball impacts normally on a surface with a spin solely around the impact velocity. One can guess that, as long as the contact between the surface and the ball remains punctual, the spin will not be altered as no torque can be applied. However, it has long been known that the ball flattens at contact. The ball and the substrate are in contact in a region of finite size, as can be observed for the quasistatic contact of a full ball with a solid substrate described by the Hertz law [15]. The same flattening is observed for hollow spheres which can even be subjected to a mechanical buckling of the shell in the contact region if the deformation is large enough [7,16,17]. Thus, in practice, the contact between the ball and the surface is not punctual and an applied torque alters the reflected angular velocity of the ball. We shall thus report on measurements of the change in the angular velocity produced by the collision between a table-tennis ball and a flat surface. In addition, we analyze the problem theoretically.

II. THEORETICAL EXPECTATIONS

When the ball enters into contact with the flat (considered rigid) surface, the ball shell deforms. It flattens in the contact region prior to being eventually subjected to a buckling instability if the impact velocity is large enough [7]. As a consequence, due to the spin of the ball, friction is at play in a finite size region, not limited to a single contact point. Let us assume that the frictional force F is applied at a distance r of the center of the contact region.

Taking the normal to the surface oriented along the z axis, the total variation of the angular velocity ω_z during the rebound can be written as

$$J \Delta\omega_z = \int_0^\tau r(t) F(t) dt, \quad (1)$$

where $J = \frac{2}{3} m R^2$ is the moment of inertia of the hollow ball (of mass m and radius R) and τ the duration of the collision. In order to obtain an estimate of the variation $\Delta\omega_z$ of the

angular velocity ω_z during the rebound, one must explicate the evolutions of $r(t)$ and $F(t)$ through time t .

Under the assumption that Coulomb's law of friction applies, the friction force F is proportional to the normal force F_N which results from the deformation of the ball during the contact with the surface. At all times, $F(t) = \mu F_N(t)$, where μ denotes the frictional coefficient. In addition, during the collision, the normal force $F_N(t)$, and thus the friction force $F(t)$, increases from 0 when the ball enters in contact with the surface, reaches its maximum value when the deformation is maximum and then returns to 0 when the ball leaves the surface.

Note that the radius $r(t)$ at which the force $F(t)$ is effectively applied is also intrinsically linked to the deformation of the ball shell and thus follows a similar temporal evolution. For instance, for the Hertz contact [15], the radius $a(t)$ of the contact area scales like $F_N^{1/3}(t)$. Here, assuming for the sake of simplicity that the normal force is homogeneously distributed over the surface of contact, we get $r(t) = \frac{2}{3} a(t)$ and, thus, $r(t) \propto F_N^{1/3}(t)$. It is worth noting that the latter relation does not apply, especially when the ball shell is subjected to the buckling instability [7]. However, the general feature that both $r(t)$ and $F(t)$ simultaneously increase and then decrease during the collision still holds. For convenience, we thus rewrite Eq. (1) in the form $J \Delta\omega_z = \bar{r} \bar{F} \tau$, where \bar{F} denotes an estimate of the magnitude of the frictional force and \bar{r} an estimate of the radius at which it is applied on average over the duration of the collision.

Without considering the detailed dynamics of the rebound, one can estimate the frictional force by considering the normal force F_N which leads to the change of the normal velocity from its incident value $v_{z,i}$ to its reflected value $v_{z,r}$. On average over time, the normal force can be estimated as follows:

$$\bar{F}_N = \frac{m(1 + \epsilon_z)v_{z,i}}{\tau}, \quad (2)$$

where ϵ_z denotes the restitution coefficient of the normal linear velocity, such that $v_{z,r} = -\epsilon_z v_{z,i}$. As $\bar{F} = \mu \bar{F}_N$, we get

$$J \Delta\omega_z = -\mu \bar{r} (1 + \epsilon_z) m v_{z,i}. \quad (3)$$

From Eq. (3), we expect the variation $\Delta\omega_z$ to be proportional to the impact velocity $v_{z,i}$ and independent of the incident angular velocity $\omega_{z,i}$. We designed an experimental setup (Sec. III) in order to probe the latter theoretical hypothesis.

III. EXPERIMENTAL PRINCIPLE AND SETUP

The experiment is designed to assess the incident and reflected linear and angular velocities of a table tennis ball right before and after the rebound on a flat and horizontal rigid surface.

The first key element of the experimental setup depicted in Fig. 1 is a launcher that makes it possible to control both the initial velocity $v_{z,i}$ along the vertical (z axis) and the initial angular velocity $\omega_{z,i}$ around it. The ball (Cornilleau™, P-ball 3 stars, 4 cm in diameter, mass 2.7 g, ABS plastic) is launched downwards using a striker consisting of a vertical metal rod driven by a spring. The system is initially armed by compressing the spring. The striker rod is

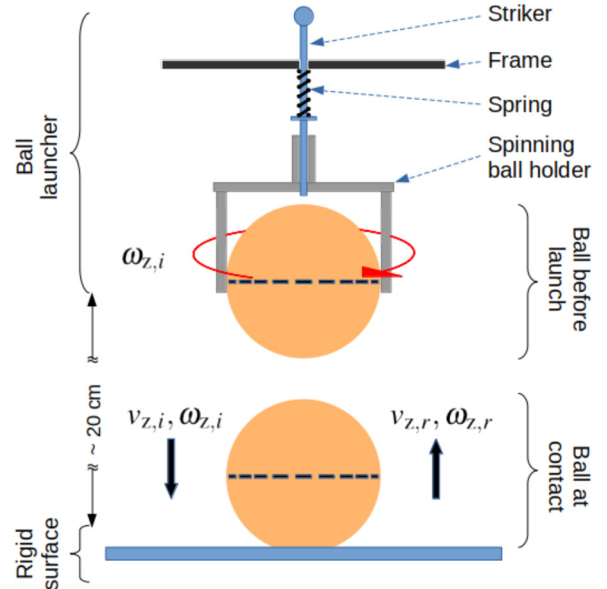


FIG. 1. Sketch of the experimental setup.

free to pass through the tubular axis of a DC motor (XD-3420, permanent magnet, 12 V). The ball is placed in a holder underneath which is attached to the motor axis. A DC power supply drives the motor permitting to prescribe the initial angular velocity $\omega_{z,i}$ up to about 300 rad s^{-1} . The striker is subsequently released. Finally, the ball reaches the solid surface (a horizontal glass window) with the vertical incident velocity $v_{z,i}$, which typically ranges from 1 m s^{-1} to 13 m s^{-1} depending on the initial compression of the spring.

The rebound of the ball is observed at 2996 fps with a fast camera (Kron Technologies, Chronos 2.1-HD, monochrome). Note that, in order to measure the angular velocity $\omega_{z,i}$, the ball joint (where the two half spheres are soldered) is assimilated to the equator and is marked with dashes (Fig. 2). Special attention is paid to initially orient the equator in the horizontal plane, thus favoring the angular velocity determination (which is achieved by measuring the horizontal velocity of the dashes) and preventing the impact from occurring within the vicinity of the joint where the local shell thickness is significantly greater. In addition, the use of the transparent glass plate makes it possible to observe the contact region, which will prove to be useful in what follows. The ball surface, in the contact region, is observed at 45 deg using the same camera at 19783 fps. For practical reasons, we use a mirror angled at 22.5 deg with respect to the vertical. The system and companion image processing protocol described in details in Ref. [7] are used here to assess the maximum radius r^m of the contact region between the ball and the substrate.

For each test, we determine the relevant characteristics of the rebound from the recorded images. In particular, since the acceleration due to gravity \vec{g} cannot be neglected, the vertical position $z(t)$ of the ball is measured as a function of time t right before and after the rebound on the glass plate. The time at contact, t_c , is given by the intersection of the two trajectories. The vertical velocities right before, $v_{z,i}$, and right

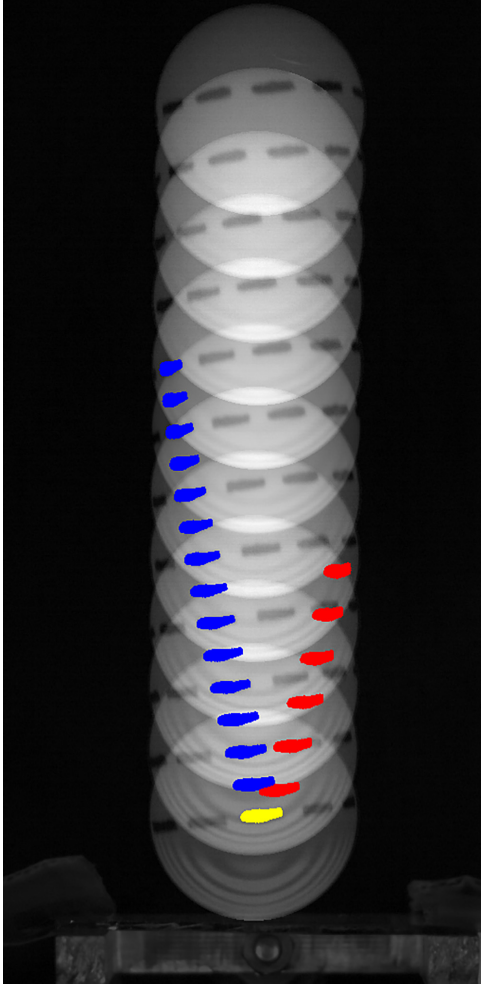


FIG. 2. Image sequence: superimposition of images of the ball after the contact. For visibility only one image out of four is displayed. Blue dashes (left) correspond to the position of one dash at the equator (one out of two positions determined experimentally). Red dashes (right) correspond to the same dash before the contact whereas the yellow dash (bottom center) corresponds to the contact ($v_{z,i} = 12 \text{ m s}^{-1}$, $\omega_{z,i} = 207 \text{ rad s}^{-1}$, 2996 fps).

after the rebound, $v_{z,r}$, are estimated from the extrapolation of the trajectories at time t_c . The angular velocities before, $\omega_{z,i}$, and after $\omega_{z,r}$ the rebound are not altered by the gravity and no significant effect of the air drag is observed over the duration (a few tens of milliseconds) of the image sequences we analyzed (Fig. 2). Values are thus averaged along the trajectories before and after the contact with the glass plate over the entire image sequence.

In the following, we focus on the variation of the angular velocity $\Delta\omega_z \equiv \omega_{z,r} - \omega_{z,i}$ as a function of the incident linear, $v_{z,i}$, and angular, $\omega_{z,i}$, velocities. However, we also determine the restitution coefficient of the linear velocity, $\varepsilon_z \equiv -\frac{v_{z,r}}{v_{z,i}}$.

IV. EXPERIMENTAL RESULTS

We first report in Fig. 3 the restitution coefficient ε_z of the normal velocity v_z for various incident impact velocities $v_{z,i}$ and angular velocities $\omega_{z,i}$. Considering

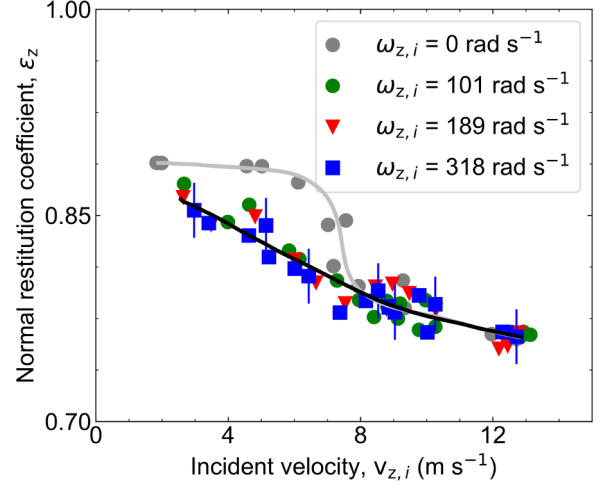


FIG. 3. Restitution coefficient ε_z vs incident velocity $v_{z,i}$. Without initial spin (gray disks), we observe two regimes: for impact velocities typically smaller than 7 m s^{-1} , ε_z only slightly decreases when $v_{z,i}$ is increased; a sudden decrease of ε_z , associated with the buckling of the ball shell, is observed for $v_{z,i}$ of about 7 m s^{-1} . By contrast, for a ball that initially spins (colored symbols), ε_z does not significantly depend on the angular velocity $\omega_{z,i}$ and a monotonic decrease of ε_z is observed when $v_{z,i}$ is increased [For the sake of clarity, gray (no spin) and black (spin) lines are drawn as guides for the eye, and error bars are indicated on a limited number of points].

the ball without initial spin ($\omega_{z,i} = 0 \text{ rad s}^{-1}$), we recover the results previously obtained as discussed in Ref. [7]. More precisely, the dependence of ε_z on $v_{z,i}$ reveals two regimes: for limited impact velocities, $v_{z,i}$ typically smaller than 7 m s^{-1} , ε_z only slightly decreases when $v_{z,i}$ increases. For larger impact velocities, a significant decrease of ε_z is observed. This behavior is accounted for by the fact that the ball shell is subjected to a buckling instability which leads to enhanced dissipation due to the friction between the two surfaces in contact [7]. When considering now the case of a ball that initially spins, we again observe that ε_z decreases when the impact velocity $v_{z,i}$ is increased. However, ε_z does not significantly depend on the initial angular velocity $\omega_{z,i}$ (in the experimental range $\omega_{z,i} \in [101, 318] \text{ rad s}^{-1}$). In addition, we remark that ε_z is systematically smaller for a spinning ball than for a ball in pure translation for $v_{z,i}$ typically smaller than 7 m s^{-1} and that the buckling instability is no longer marked by any change in regime. With this new configuration of an impinging ball spinning along its velocity axis, and unlike the case where the incident ball has no spin, friction cannot be neglected prior to buckling, and the restitution coefficient ε_z decreases continuously, without any change in regime, when the incident velocity is increased.

In Fig. 4, we report the variation of the angular velocity $\Delta\omega_z$ as a function of the incident velocity $v_{z,i}$ for various values of the initial angular velocity $\omega_{z,i}$. As expected, we observe that $\Delta\omega_z$ decreases when the impact velocity is increased. However, the variation $\Delta\omega_z$ does depend on the initial angular velocity $\omega_{z,i}$, contrary to what is naively expected from our preliminary theoretical arguments presented

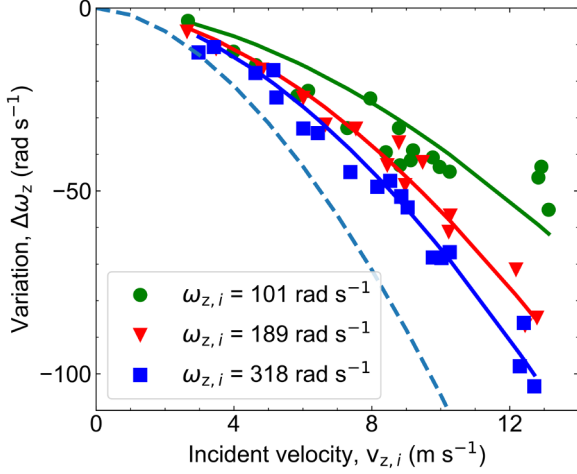


FIG. 4. Variation $\Delta\omega_z$ of the angular velocity vs incident velocity $v_{z,i}$. The variation $\Delta\omega_z$ evolves more than linearly with the impact velocity $v_{z,i}$ and does depend on the angular velocity $\omega_{z,i}$. The dotted line corresponds to the limit $\omega_{z,i} \rightarrow \infty$ (Symbols: experimental data. Lines: Eq. (6) with $m = 2.7g$, $\epsilon_z = 0.8$, $\mu = 0.22$, $\tau = 0.6$ ms, $a \simeq 0.74$, and $b \simeq 0.085$).

in Sec. II. This observation is the key result of the present study.

V. DISCUSSION

A physical ingredient is clearly missing in Sec. II for the model to account for the dependence of $\Delta\omega_z$ on the initial spin $\omega_{z,i}$, dependence which does not appear in Eq. (3).

We already mentioned that the ball shell deforms throughout the contact. It is thus interesting to consider the displacement of the ball shell with respect to the solid flat surface. The problem is complex as the ball deformation can result in a buckling instability. However, the effect of the initial flattening of the shell, previous to an eventual buckling, can still be studied. The ball shell flattens in the contact region leading to a compression of the shell in the contact plane. The initially spherical shell (of radius $R = 2$ cm) becomes a flat disk in a region of radius r^m , typically. Considering the change in the surface area, we estimate that the average local strain ϵ_{rr} is of the order of $\epsilon_{rr} \sim \frac{1}{8}(\frac{r^m}{R})^2$. Thus a point of the shell at a distance r from the center of the contact region is displaced by a distance of the order of $r\epsilon_{rr}$ with respect to the flat surface. At the distance \bar{r} this induces a radial displacement $\bar{r}\epsilon_{rr}$ during the time $\tau/2$. Consequently the relative radial velocity v_r of the two solid surfaces in regard equals $2\bar{r}\epsilon_{rr}/\tau$, which was previously neglected.

In order to estimate v_r , let us first report on the maximum external radius of the contact region r^m as a function of the incident velocity $v_{z,i}$ (Fig. 5). Within the experimental conditions explored, the typical radius is of about 5 mm. Thus, assuming that \bar{r} is of the order of r^m and taking into account the typical duration of the contact between the ball and the glass substrate, $\tau = 0.6$ ms [7], we get that v_r is of the order of 0.1 m s⁻¹. The latter value must be compared to the typical orthoradial velocity v_o , due to the angular velocity ω_z at the

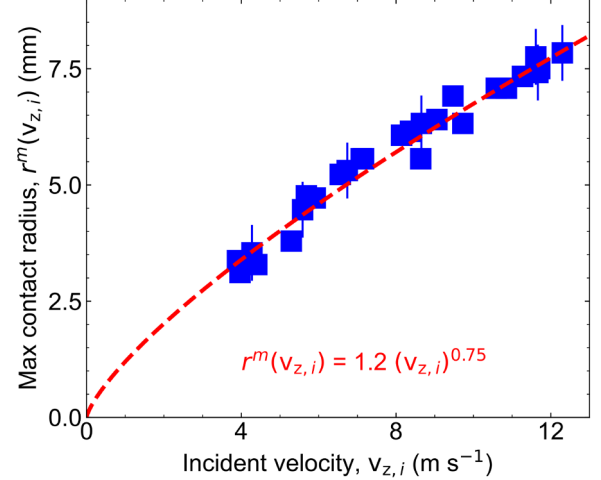


FIG. 5. Maximum external radius r^m of the contact region vs incident velocity $v_{z,i}$. The increase in the maximum radius of the contact region as a function of the incident velocity is well accounted for by a power law (Symbols: experimental data. Line: interpolation by a power law).

distance \bar{r} of the center of the contact region. Assuming again that \bar{r} is of the order of r^m , one gets $v_o \sim r^m \omega_z \sim 1$ m s⁻¹ for $\omega_z \sim 200$ rad s⁻¹, an intermediate value of the angular velocity. As a conclusion, the radial velocity v_r is a fraction of the orthoradial velocity v_o and this component cannot be neglected.

As a consequence of the combination of the two velocity components, namely the radial, v_r , and orthoradial, v_o , velocities, the resulting friction force μF_N , which applies at a distance r from the center of the contact zone, is no longer purely orthoradial but makes the angle α with the orthoradial direction (Fig. 6) :

$$\cos \alpha = \frac{v_o}{\sqrt{v_r^2 + v_o^2}}. \quad (4)$$

The angle α depends on time t and we are unable to assess experimentally the radial velocity v_r . However, in order to prove that the proposed physical ingredients are correct, we can estimate the variation of the angular velocity by writing

$$J \Delta\omega_z = \bar{r} \cos \alpha \mu \bar{F}_N \tau, \quad (5)$$

where estimates of r , α , and the normal force F_N on average over the contact time τ are used. Note that in the case of $\alpha = 0$ we come back to the previous simplified case depicted by Eq. (3). As in Sec. II, we take $\bar{F}_N \tau \simeq (1 + \epsilon_z) m v_{z,i}$ [Eq. (2)]. We suggest that the typical radius at which the friction force is applied is a fraction a of maximum radius r^m , i.e., $\bar{r} = a r^m$, that the typical orthoradial velocity $v_o = \bar{r} \omega_{z,i}$, and, finally, that the typical radial velocity of the shell material in contact with the substrate is a fraction b of r^m/τ , i.e., $v_r = b r^m/\tau$. With these estimates, and the resulting estimate of $\cos(\alpha)$, we get

$$J \Delta\omega_z \simeq -a \mu [(1 + \epsilon_z) m v_{z,i}] r^m \frac{\tau \omega_{z,i}}{\sqrt{b^2 + (\tau \omega_{z,i})^2}}. \quad (6)$$

Qualitatively Eq. (6) accounts for a larger variation of the angular velocity when both the impact velocity and the

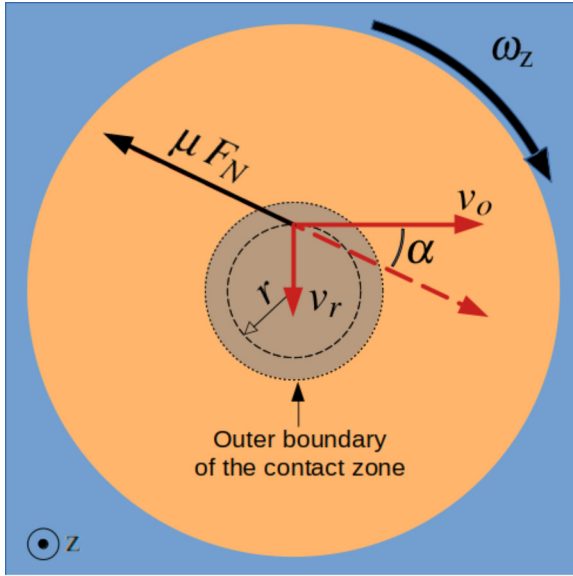


FIG. 6. Top view of the contact region. Due to the rapid variation of the contact region radius from 0 to r^m , back and forth during the time τ , the friction force μF_N is not orthoradial but rather makes a finite angle α with the orthoradial direction. The torque reducing the ball angular velocity is thus smaller than expected in the absence of radial sliding.

angular velocity are increased. This equation is in a good agreement with the experimental results reported in Fig. 4. For a given incident velocity $v_{z,i}$, the maximum variation $\Delta\omega_z$ is reached in the limit $\omega_{z,i} \rightarrow \infty$ (dashed line in Fig. 4), when the radial velocity v_r is small compared to the orthoradial velocity v_o ($\alpha \rightarrow 0$ in Fig. 6). Within the experimental range of angular velocity, this limit is never reached but is approached when $\omega_{z,i}$ is increased.

Quantitatively, the interpolation of the experimental data reported in Fig. 5 gives $r^m \simeq 1.2 \cdot 10^{-3} v_{z,i}^{3/4}$ m, which leads to $\Delta\omega_z \propto v_{z,i}^{7/4}$, typically. Having in mind that a denotes the fraction of the maximum radius r^m at which the friction force is applied ($\bar{r} = a r^m$), and b the fraction of the velocity r^m/τ which accounts for the radial velocity v_r ($v_r = b r^m/\tau$), we expect a to be of the order of a few tenths whereas b must be much smaller. In order to go further, we note that the restitution coefficient of the normal velocity only slowly depends on the impact velocity and is independent of the initial spin (Fig. 3). With the value $\epsilon_z = 0.8$ at intermediate incident velocity, $\mu = 0.22$ and $\tau = 0.6$ ms [7,18], the best agreement of Eq. (6) with the experimental data is obtained for $a \simeq 0.74$ and $b \simeq 0.085$ (solid lines in Fig. 4).

On the one hand, a accounts for the effective radius at which the maximum friction force F_N is applied. For the sake for simplicity, let us neglect the radial velocity v_r (i.e., $\alpha = 0$) and assume that $\epsilon_z = 1$. Assuming further that both the radius r and the force evolve sinusoidally in time, thus writing $r(t) = r^m \sin(\Omega t)$ and $F(t) = \mu m \Omega v_{z,i} \sin(\Omega t)$, we integrate the dynamical equation Eq. (1) and get $a = \frac{\pi}{4} \simeq 0.78$, which is in rather good agreement with the experimental value $a \simeq 0.74$. On the other hand, if the radial displacement due to the flattening of the ball shell is accounted for, we

expect $v_r = b r^m/\tau = 2\bar{r}\epsilon_{rr}/\tau$. For the intermediate value $r^m = 5$ mm, we estimate that $\epsilon_{rr} \sim 8 \times 10^{-3}$ and thus that $b \sim 0.012$ smaller than but of the same order of magnitude as the experimental value $b \simeq 0.085$ in this case. However this estimate must be considered with care as it is obtained by considering a simple flattening of the shell in the contact region, excluding the deformation of the entire ball as well as its possible buckling.

All in all, the proposed model seems to contain the essential physical ingredients that explain the dependence of the variation of the angular velocity on both the incident velocity and spin.

VI. CONCLUSION

The rebound of a table-tennis ball, spinning around its linear velocity vector, colliding in normal incidence with a flat and rigid surface, is of peculiar interest because this is one specific situation in which the various components of the velocity are necessarily coupled in a nonlinear manner. Indeed, the change in the angular velocity around the normal to the surface depends not only on the impact velocity but also on the associated spatial extension of the contact region.

The present experimental study reveals the complexity of the problem. Indeed, even if part of the nonlinearity arises from the dependence of the size of the contact region on the impact velocity, the effect on the orientation of the frictional force was not expected. The simple theoretical analysis that complements the study, together with the former studies in [7–9,19,20], now provides a complete theoretical description of the laws governing the rebound of a table-tennis ball, and more generally of sport balls, on a solid substrate. Indeed, it has been previously observed that the restitution coefficient of the normal velocity is mostly independent of the incidence angle, in spite of a small dependence on the normal velocity itself [7]. The oblique impact is well understood which leads to relations between the in-plane linear and angular velocities before and after the collision [8–10,18]. The present work gives an estimate of the angular velocity around the normal to the surface, which was the last element missing to provide all the spin and velocity components after rebound. Now, for any rotation, velocity, and angle of incidence, we can decompose spin and velocity into their components normal and parallel to the surface and, with friction properly taken into account, we can propose a general law of rebound [18].

The full description of the rebound applies to the ball impinging on the table, assumed rigid. A natural extension of the study will be to analyze the rebound on a deformable polymeric surface such as the coating of the table-tennis paddle. It has been attempted under normal incidence with no spin [21] and under oblique incidence with spin parallel to the surface [22], using numerical simulations, yet evidencing the need for a more general framework.

ACKNOWLEDGMENTS

T.R. gratefully acknowledges the GDR Sport & Activit  Physique for its financial support. The authors also thank F. Vittoz for setting up the experimental device.

- [1] H. M. Jaeger, S. R. Nagel, and R. P. Behringer, Granular solids, liquids, and gases, *Rev. Mod. Phys.* **68**, 1259 (1996).
- [2] H. Brody, That's how the ball bounces, *Phys. Teacher* **22**, 494 (1984).
- [3] R. Cross, Impact of a ball with a bat or racket, *Am. J. Phys.* **67**, 692 (1999).
- [4] R. Cross, The bounce of a ball, *Am. J. Phys.* **67**, 222 (1999).
- [5] R. Cross, The coefficient of restitution for collisions of happy balls, unhappy balls, and tennis balls, *Am. J. Phys.* **68**, 1025 (2000).
- [6] H. Brody, Bounce of a tennis ball, *J. Sci. Med. Sport* **6**, 113 (2003).
- [7] T. Rémond, V. Dolique, F. Vittoz, S. Antony, R. G. Rinaldi, L. Manin, and J.-C. Géminard, Dynamical buckling of a table-tennis ball impinging normally on a rigid target: Experimental and numerical studies, *Phys. Rev. E* **106**, 014207 (2022).
- [8] R. Cross, Grip-slip behavior of a bouncing ball, *Am. J. Phys.* **70**, 1093 (2002).
- [9] R. Cross, Measurements of the horizontal coefficient of restitution for a superball and a tennis ball, *Am. J. Phys.* **70**, 482 (2002).
- [10] T. Rémond, V. Dolique, R. G. Rinaldi, and J.-C. Géminard, Oblique impact of a buckling table-tennis ball on a rigid surface, *Phys. Rev. E* **107**, 055007 (2023).
- [11] S. R. Goodwill and S. J. Haake, Ball spin generation for oblique impacts with a tennis racket, *Exp. Mech.* **44**, 195 (2004).
- [12] W. J. Stronge and A. D. C. Ashcroft, Oblique impact of inflated balls at large deflections, *Int. J. Impact Eng.* **34**, 1003 (2007).
- [13] C. Y. Wu, C. Thornton, and L. Y. Li, A semi-analytical model for oblique impacts of elastoplastic spheres, *Proc. R. Soc. A.* **465**, 937 (2009).
- [14] T. Allen, S. Haake, and S. Goodwill, Effect of friction on tennis ball impacts, *Proc. Inst. Mech. Eng. Part: J. Sport Eng. Technol.* **224**, 229 (2010).
- [15] H. Hertz, Über die berührung fester elastischer körper, *J. Reine Angew. Math.* **92**, 156 (1881).
- [16] L. Pauchard and S. Rica, Contact and compression of elastic spherical shells: The physics of a 'ping-pong' ball, *Philos. Mag. B* **78**, 225 (1998).
- [17] S. Knoche and J. Kierfeld, Buckling of spherical capsules, *Phys. Rev. E* **84**, 046608 (2011).
- [18] T. Rémond, *Physique du rebond: application à la balle de tennis de table*, Ph.D. thesis, Ecole Normale Supérieure de Lyon, 2023.
- [19] M. Hubbard and W. Stronge, Bounce of hollow balls on flat surfaces, *Sports Eng.* **4**, 49 (2001).
- [20] H. Dong and M. Moys, Experimental study of oblique impacts with initial spin, *Powder Technol.* **161**, 22 (2006).
- [21] R. G. Rinaldi, L. Manin, C. Bonnard, A. Drillon, H. Lourenco, and N. Havard, Non linearity of the ball/rubber impact in table tennis: experiments and modeling, *Procedia Eng.* **147**, 348 (2016).
- [22] R. G. Rinaldi, L. Manin, S. Moineau, and N. Havard, Table tennis ball impacting racket polymeric coatings: Experiments and modeling of key performance metrics, *Appl. Sci.* **9**, 158 (2019).